Partition functions for complex fugacity

Part I

Barry M. McCoy

CN Yang Institute of Theoretical Physics

State University of New York,

Stony Brook, NY, USA

In collaboration with

Michael Assis, Stony Brook University

Jesper Jacobsen, ENS Paris

Iwan Jensen, University of Melbourne

Jean-Marie Maillard, University of Paris VI

Based in part on "Hard hexagon partition function for complex fugacity" arXiv: 1306.6389

Motivation

In 1999-2000 Nickel discovered and in 2001 Orrick, Nickel, Guttmann and Perk extensively analyzed the evidence for a natural boundary in the susceptibility of the Ising model in the complex temperature plane.

This present study is an attempt to understand the implications of this discovery.

Outline

1. Problems for complex fugacity
2. Preliminaries for hard hexagons and squares
3. Hard hexagon analytic results
4. Hard hexagon equimodular curves
5. Hard hexagon partition function zeros
6. Hard square zeros
7. Ising in a field
8. Further open questions
9. Conclusion

1. Problems for complex fugacity

1. Existence of a shape independent partition function per site.
2. Equimodular curves versus partition function zeros
3. Areas versus curves of zeros
4. Analytic continuation versus natural boundaries
5. Integrable versus generic non-integrable systems

2. Preliminaries for hard hexagons and squares

1. Grand partition function on an $L_v \times L_h$ lattice
$Z_{L_v,L_h}(z) = \sum_{N=0}^{\infty} g(N) \cdot z^N$
where $g(N)$ is the number of allowed configurations.

2. Transfer matrices
$T_{\{b_1,\cdots b_{L_h}\},\{a_1,\cdots.a_{L_h}\}} = \prod_{j=1}^{L_h} W(a_j,\, a_{j+1};\, b_j,\, b_{j+1})$
where the occupation numbers a_j, b_j take the values $0, 1$ with

3. Boltzmann weights

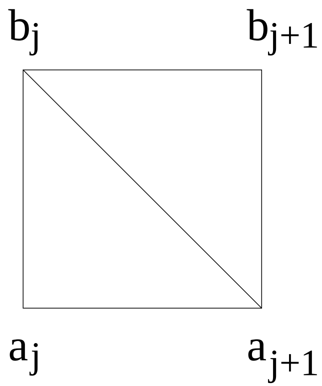

For hard squares

$W(a_j, a_{j+1}; b_j, b_{j+1}) = 0$ for
$a_j a_{j+1} = b_j b_{j+1} = a_j b_j = a_{j+1} b_{j+1} = 1,$
and otherwise:
$W(a_j, a_{j+1};\ b_j, b_{j+1}) = z^{(a_j + a_{j+1} + b_j + b_{j+1})/4}$

For hard hexagons

$W(a_j, a_{j+1}; b_j, b_{j+1}) = 0$ for
$a_j a_{j+1} = b_j b_{j+1} = a_j b_j = a_{j+1} b_{j+1} = a_{j+1} b_j = 1,$
and otherwise:
$W(a_j, a_{j+1};\ b_j, b_{j+1}) = z^{(a_j + a_{j+1} + b_j + b_{j+1})/4}$

4. Partition functions from transfer matrices eigenvalues

For toroidal boundary conditions

$$Z^T_{L_v,L_h}(z) = \mathrm{Tr} T^{L_v}(z;L_h) = \sum_k \lambda_k^{L_v}(z;L_h)$$

For cylindrical boundary conditions

$$Z^C_{L_v,L_jh}(z) = \langle \mathbf{v}|T^{L_v}(z;L_h)|\mathbf{v}\rangle = \sum_k \lambda_k^{L_v}(z;L_h)c_k$$

with

$\mathbf{v}(a_1, a_2. \cdots, a_{L_h}) = \prod_{j=1}^{L_h} z^{a_j/2}$ and

$c_k = (\mathbf{v}\cdot\mathbf{v}_k)(\mathbf{v}_k\cdot\mathbf{v})$

where λ_k are eigenvalues and $\mathbf{v}_k$ are eigenvectors

For hard squares $T = T^t$; λ_k real for real z

For hard hexagons $T \neq T^t$; some λ_k complex for real z

5. Thermodynamic limit

For thermodynamics to be valid we must have
$F/k_BT = \lim_{L_v,L_h\to\infty}(L_vL_h)^{-1}\ln Z_{L_v,L_h}(z)$
independent of the aspect ratio L_v/L_h.

In terms of the transfer matrix eigenvalues
$\lim_{L_v\to\infty} L_v^{-1}\ln Z_{L_v,L_h}(z) = \ln\lambda_{\max}(z;L_h)$

Therefore if

$$\lim_{L_h\to\infty} L_h^{-1}\lim_{L_v\to\infty} L_v^{-1}\ln Z_{L_v,L_h}(z) = \lim_{L_v,L_h\to\infty}(L_vL_h)^{-1}\ln Z_{L_v,L_h}(z)$$

then
$-F/k_BT = \lim_{L_h\to\infty} L_h^{-1}\ln\lambda_{\max}(z;L_h)$
For $z\geq 0$ this independence is rigorously true in general. For complex z there is no general proof and for hard squares for $z=-1$ it is known to be false.

6. Partition function zeros versus equimodular curves

We begin with the simplest case where
$L_v \to \infty \quad \text{with} \quad L_h \quad \text{fixed}$
where the aspect ratio $L_v/L_h \to \infty$.

The zeros will lie on curves where two or more transfer matrix eigenvalues have equal modulus
$|\lambda_1(z; L_h)| = |\lambda_2(z; L_h)|$
On this curve $\frac{\lambda_1(z;L_h)}{\lambda_2(z;L_h)} = e^{i\phi(z)} \quad \text{with } \phi(z) \text{ real.}$
The density of zeros on this curve is proportional to $d\phi(z)/dz$

The cases of cylindrical and toroidal boundary conditions have distinct features which must be treated separately.

Cylindrical boundary conditions

Because the boundary vector $\mathbf{v}$ is translationally invariant only eigenvectors in the sector $P = 0$ will have non vanishing scalar products $(\mathbf{v} \cdot \mathbf{v}_k)$. All equimodular curves have only two equimodular eigenvalues.

Toroidal boundary conditions

In this case all eigenvalues contribute. The eigenvalues for P and $-P$ have equal modulus because of translational invariance and thus on equimodular curves there can be either 2, 3, or 4 equimodular eigenvalues.

3. Hard hexagon analytic results

Baxter in 1980 has computed the fugacity z and the partition function per site

$\kappa_{\pm}(z) = \lim_{L_h\to\infty} \lambda_{\max}(z; L_h)^{1/L_h}$

for positive z terms of an auxiliary variable x using the functions

$$G(x) = \prod_{n=1}^{\infty} \frac{1}{(1-x^{5n-4})(1-x^{5n-1})}$$
$$H(x) = \prod_{n=1}^{\infty} \frac{1}{(1-x^{5n-3})(1-x^{5n-2})}$$
$$Q(x) = \prod_{n=1}^{\infty} (1-x^{n}).$$

There are two regimes $0 \leq z \leq z_c \leq z \leq \infty$ where

$z_c = \frac{11+5\sqrt{5}}{2} = 11.090169\cdots$

Both $\kappa_{\pm}(z)$ have singularities only at

$z_c, \quad z_d = -1/z_c = -0.090169\cdots, \quad \infty.$

Partition functions per site

High density $z_c < z < \infty$

$$z = \frac{1}{x} \cdot \left(\frac{G(x)}{H(x)}\right)^5$$

$$\kappa_+ \; = \; \frac{1}{x^{1/3}} \cdot \frac{G^3(x)\,Q^2(x^5)}{H^2(x)} \cdot \prod_{n=1}^{\infty} \frac{(1-x^{3n-2})(1-x^{3n-1})}{(1-x^{3n})^2}$$

where, as x increases from 0 to 1, the value of z^{-1} increases from 0 to z_c^{-1}.

Low density $0 < z < z_c$

$$z = -x \cdot \left(\frac{H(x)}{G(x)}\right)^5$$

$$\kappa_- = \frac{H^3(x)\,Q^2(x^5)}{G^2(x)} \cdot \prod_{n=1}^{\infty} \frac{(1-x^{6n-4})(1-x^{6n-3})^2(1-x^{6n-2})}{(1-x^{6n-5})(1-x^{6n-1})(1-x^{6n})^2},$$

where, as x decreases from 0 to -1, the value of z increases from 0 to z_c.

Algebraic equation for $\kappa_+(z)$

Both $\kappa_\pm(z)$ are algebraic functions of z. Joyce in 1987 obtained the equation for $\kappa_+(z)$ using the polynomials

$$\Omega_1(z) = 1 + 11z - z^2$$
$$\Omega_2(z) = z^4 + 228z^3 + 494z^2 - 228z + 1$$
$$\Omega_3(z) = (z^2+1)\cdot(z^4 - 522z^3 - 10006z^2 + 522z + 1).$$

$$f_+(z,\kappa_+) = \sum_{k=0}^4 C_k^+(z)\kappa_+^{6k} = 0, \quad \text{where}$$

$$C_0^+(z) = -3^{27}\,z^{22}$$
$$C_1^+(z) = -3^{19}z^{16}\cdot\Omega_3(z)$$
$$C_2^+(z) = -3^{10}z^{10}\cdot[\Omega_3^2(z) - 2430z\cdot\Omega_1^5(z)]$$
$$C_3^+(z) = -z^4\cdot\Omega_3(z)\cdot[\Omega_3^2(z) - 1458\,z\cdot\Omega_1^5(z)]$$
$$C_4^+(z) = \Omega_1^{10}(z).$$

Algebraic equation for $\kappa_-(z)$

For low density we have obtained by means of a Maple computation the algebraic equation for $\kappa_-(z)$ $f_-(z,\kappa_-) = \sum_{k=0}^{12} C_k^-(z) \cdot \kappa_-^{2k} = 0$, where

$$C_0^-(z) = -2^{32} \cdot 3^{27} \cdot z^{22}$$
$$C_1^-(z) = 0$$
$$C_2^-(z) = 2^{26} \cdot 3^{23} \cdot 31 \cdot z^{18} \cdot \Omega_2(z),$$
$$C_3^-(z) = 2^{26} \cdot 3^{19} \cdot 47 \cdot z^{16} \cdot \Omega_3(z),$$
$$C_4^-(z) = -2^{17} \cdot 3^{18} \cdot 5701 \cdot z^{14} \cdot \Omega_2^2(z),$$
$$C_5^-(z) = -2^{16} \cdot 3^{14} \cdot 7^2 \cdot 19 \cdot 37 \cdot z^{12} \cdot \Omega_2(z)\,\Omega_3(z),$$
$$C_6^-(z) = -2^{10} \cdot 3^{10} \cdot 7 \cdot z^{10} \cdot [273001 \cdot \Omega_3^2(z) + 2^6 \cdot 3^5 \cdot 5 \cdot 4933 \cdot z \cdot \Omega_1^5(z)],$$
$$C_7^-(z) = -2^9 \cdot 3^{10} \cdot 11 \cdot 13 \cdot 139 \cdot z^8 \cdot \Omega_3(z)\,\Omega_2^2(z),$$
$$C_8^-(z) = -3^5 \cdot z^6 \cdot \Omega_2(z) \cdot [7 \cdot 1028327 \cdot \Omega_3^2(z) - 2^6 \cdot 3^4 \cdot 11 \cdot 419 \cdot 16811 \cdot z \cdot \Omega_1^5(z)],$$
$$C_9^-(z) = -z^4 \cdot \Omega_3(z) \cdot [37 \cdot 79087\,\Omega_3^2(z) + 2^6 \cdot 3^6 \cdot 5150251 \cdot z \cdot \Omega_1^5(z)],$$
$$C_{10}^-(z) = -z^2 \cdot \Omega_2^2(z) \cdot [19 \cdot 139\Omega_3^2(z) - 2 \cdot 3^6 \cdot 151 \cdot 317 \cdot z \cdot \Omega_1^5(z)]$$
$$C_{11}^-(z) = -\Omega_2(z)\,\Omega_3(z) \cdot [\Omega_3^2(z) - 2 \cdot 613 \cdot z \cdot \Omega_1^5(z)],$$
$$C_{12}^-(z) = \Omega_1^{10}(z).$$

Analyticity of $\kappa_{\pm}(z)$

High density

$\kappa_+(z)$ is real and positive for $z_c < z < \infty$
For $z \to \infty$
$\kappa_+(z) = z^{1/3} + \frac{1}{3}z^{-2/3} + \frac{5}{9}z^{-5/3} + \cdots$
$\kappa_+(z)$ is analytic in the plane cut from $-\infty < z < z_c$

On the segment $-\infty < z < z_d$ $\kappa_+(z)$ has the phase $e^{\pm\pi i/3}$ for $\mathrm{Im} z = \pm\epsilon \to 0$.

Low density

κ_- is real and positive for $z_d < z < z_c$
κ_- is analytic in the plane cut from $z_c < z < \infty$ and $-\infty < z < z_d$

Values of $\kappa_\pm(z)$ at z_c and z_d

At z_c

$$(w_{c+} + 3^9)^3 = 0 \quad \text{with} \quad w_{c+} = -(5^{5/2}/z_c)^3 \kappa_+^6(z_c)$$

$$(w_{c-} + 2^4)^2 \cdot (w_{c-} - 3^3)^3 \cdot (w_{c-} - 2^4 \cdot 3^3)^6 = 0$$

$$\text{with} \quad w_{c-} = 5^{5/2} \kappa_-^2(z_c)/z_c$$

At $z = z_d$

$$(w_{d+} + 3^9)^3 = 0 \quad \text{with} \quad w_{d+} = -(5^{5/2}/z_d)^3 \kappa_+^6(z_d)$$

$$(w_{d-} - 2^4)^2 \cdot (w_{d-} + 3^3)^3 \cdot (w_{d-} + 2^4 \cdot 3^3)^6 = 0$$

$$\text{with} \quad w_{d-} = 5^{5/2} \kappa_-^2(z_d)^2/z_d$$

Thus using appropriate boundary conditions

$$\kappa_+(z_c) = \kappa_-(z_c) = (3^3 \cdot 5^{-5/2}\, z_c)^{1/2} = 2.3144003\cdots$$

$$\kappa_+(z_d) = e^{\pm\pi i/3} 0.208689, \quad \kappa_-(z_d) = 4|\kappa_+(z_d)|$$

Expansion of $\rho_{-}(z)$ at z_d

Joyce obtained an algebraic equation for the low density density function $\rho_{-}(z)$ and expanded it at z_c. We have obtained the expansion at z_d as

$$\rho_{-}(z) = t_d^{-1/6}\Sigma_0(t_d) + \Sigma_1(t_d) + t_d^{2/3}\Sigma_2(t_d) + t_d^{3/2}\Sigma_3(t_d) + t_d^{7/3}\Sigma_4(t_d) + t_d^{19/6}\Sigma_5(t_d)$$

where $t_d = 5^{-3/2}(1 - z/z_d)$

$$\Sigma_0 = -\frac{1}{\sqrt{5}} + \frac{1}{12}\left(5 + \frac{11}{\sqrt{5}}\right)t_d + \frac{1}{144}\left(275 + \frac{639}{\sqrt{5}}\right)t_d^2 + \frac{1}{1296}\left(17765 + \frac{37312}{\sqrt{5}}\right)t_d^3 + \cdots$$

$$\Sigma_1 = \frac{1}{2}\left(1 + \frac{1}{\sqrt{5}}\right) + \frac{1}{\sqrt{5}}t_d + \frac{1}{2}\left(5 - \frac{1}{\sqrt{5}}\right)t_d^2 - \frac{1}{2}\left(5 - \frac{83}{\sqrt{5}}\right)t_d^3 + \cdots$$

$$\Sigma_2 = -\frac{2}{\sqrt{5}} - \frac{2}{15}(25 - 4\sqrt{5})t_d + \frac{4}{45}(125 - 108\sqrt{5})t_d^2 - \frac{4}{405}(16775 - 4621\sqrt{5})t_d^3 + \cdots$$

$$\Sigma_3 = -\frac{3}{\sqrt{5}} - \frac{3}{4}\left(15 - \frac{7}{\sqrt{5}}\right)t_d + \frac{3}{16}\left(175 - \frac{1189}{\sqrt{5}}\right)t_d^2 - \frac{21}{16}\left(705 - \frac{646}{\sqrt{5}}\right)t_d^3 + \cdots$$

$$\Sigma_4 = -\frac{4}{\sqrt{5}} - \frac{2}{15}(175 - 13\sqrt{5})t_d + \frac{2}{45}(1625 - 2637\sqrt{5})t_d^2 - \frac{52}{405}(22100 - 3499\sqrt{5})t_d^3 + \cdots$$

$$\Sigma_5 = -\frac{6}{\sqrt{5}} - \frac{1}{2}\left(95 - \frac{31}{\sqrt{5}}\right)t_d + \frac{1}{24}\left(3875 - \frac{34641}{\sqrt{5}}\right)t_d^2 - \frac{31}{216}\left(55685 - \frac{40892}{\sqrt{5}}\right)t_d^3 + \cdots$$

The term in $t_d^{2/3}$ was first obtained by Dhar but the full expansion has not been previously reported.

comments

All six infinite series converge.
The form follows from the renormalization group expansion of the singular part of the free energy at $z = z_d$

$$f_s = t_d^{2/y} \cdot \sum_{n=0}^{4} t_d^{-n(y'/y)} \cdot \sum_{m=0}^{\infty} a_{n;m} \cdot t_d^m.$$

$y = 12/5$ is the leading renormalization group exponent for the Yang-Lee edge which is equal to ν^{-1} (the inverse of the correlation length exponent). The exponent ν at z_d has never been directly computed.

$y' = -2$ is the exponent for the contributing irrelevant operator which breaks rotational invariance on the triangular lattice.

Factorization of the characteristic equation

For a transfer matrix with cylindrical boundary conditions the characteristic equation factorizes into subspaces characterized by a momentum eigenvalue P. In general the characteristic polynomial in the translationally invariant $P = 0$ subspace will be irreducible. We have found that this is indeed the case for hard squares. However, for hard hexagons we find that for $L_h = 12, 15, 18$, the characteristic polynomial, for $P = 0$, factors into the product of two irreducible polynomials with integer coefficients. We have not been able to study the factorization for larger values of L_h but we presume that factorization always occurs and is a result of the integrability of hard hexagons. What is unclear is if for larger lattices a factorization into more than two factors can occur.

Multiplicity of the roots of the resolvent

An even more striking non-generic property of hard hexagons is seen in the computation of the resultant of the characteristic polynomial in the translationally invariant sector. The zeros of the resultant locate the positions of all potential singularities of the polynomials.

We have been able to compute the resultant for $L_h = 12, 15, 18$, and find that almost all zeros of the resultant have multiplicity two which indicates that there is in fact no singularity at the point and that the two eigenvalues cross. This very dramatic property will almost certainly hold for all L_h and must be a consequence of the integrability (although to our knowledge no such theorem is in the literature).

The equimodular curve $|\kappa_-(z)| = |\kappa_+(z)|$

If the two eigenvalues $\kappa_-(z)$ and $\kappa_+(z)$ were sufficient to describe the partition function in the entire complex z plane then there will be zeros on the equimodular curve $|\kappa_-(z)| = |\kappa_+(z)|$. An algebraic expression for this curve can be obtained but in practice it is too large to use. Instead we have numerically computed the curve from the parametric expressions of Baxter.

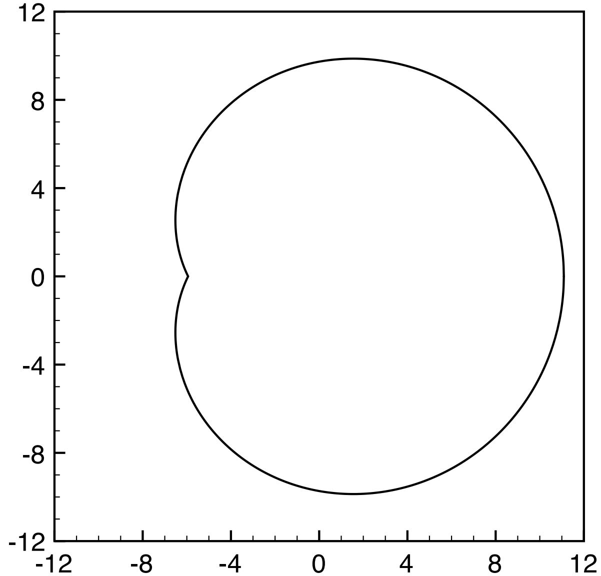

4. Hard hexagon equimodular curves

We have numerically computed equimodular curves for systems up to size $L_h = 30$. We have restricted our attention to $L_h/3$ an integer which is commensurate with hexagonal ordering in the high density phase.

For cylindrical boundary conditions only eigenvalues with $P = 0$ contribute to the partition function.

For toroidal boundary conditions all momentum sectors contribute. This is particularly important because in the ordered phase there are eigenvalues with $P = \pm 2\pi/3$ which for real z are asymptotically degenerate in modulus with the $P = 0$ maximum eigenvalue.

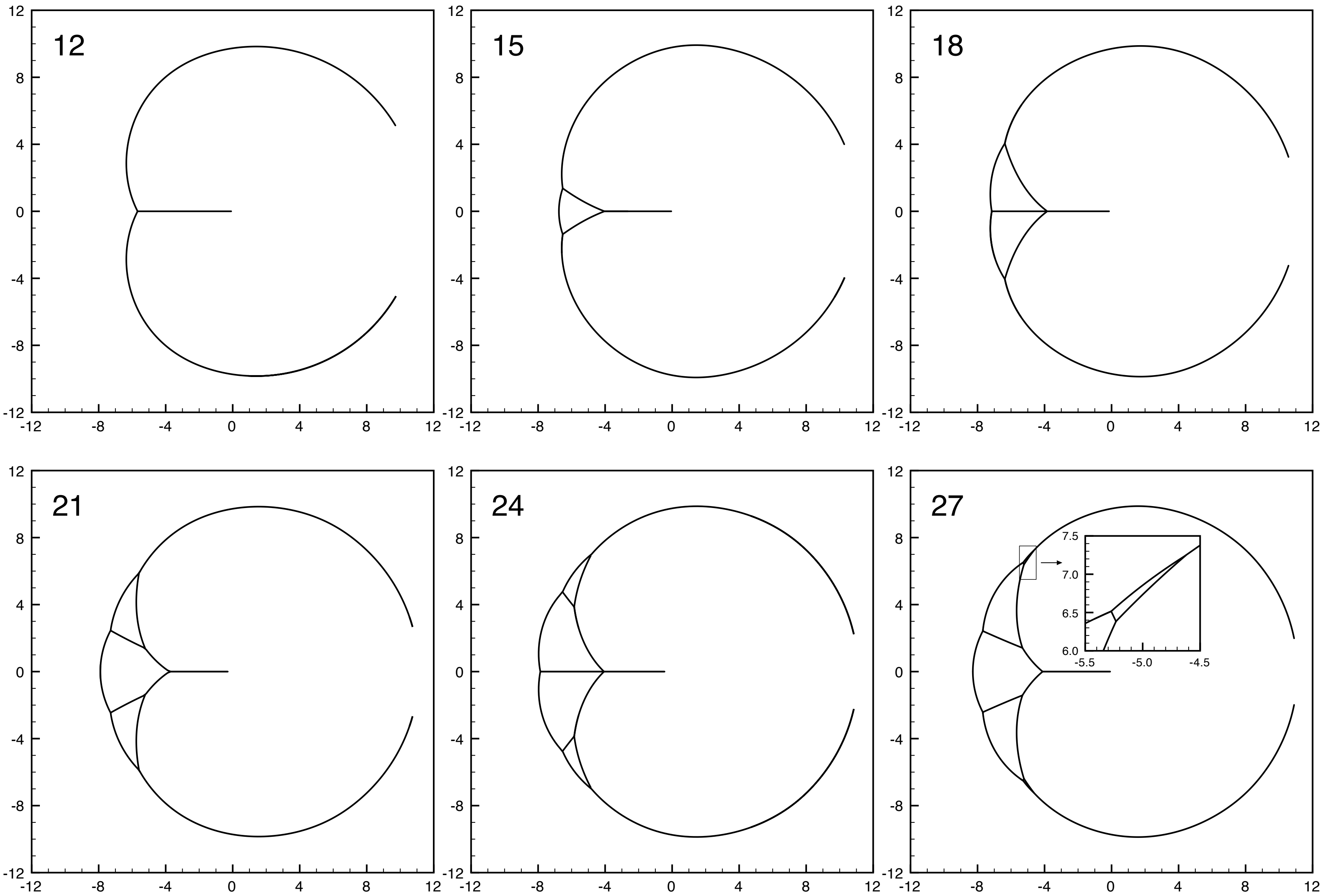

Hard hexagon equimodular curves with cylindrical boundary conditions with $P = 0$.

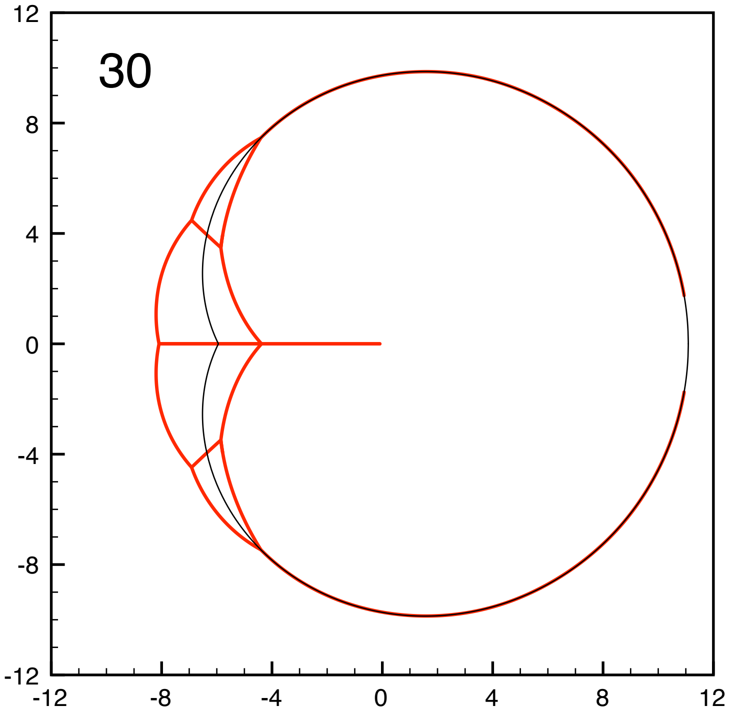

Comparison of the dominant eigenvalue crossings $L_h = 30$ in red with $|\kappa_+(z)| = |\kappa_-(z)|$ in black.

Comments

1. There are no gaps in these curves. This is a consequence of the resolvent having double roots. We will see that hard squares are very different.

2. The right side of all the plots is extremely well fit by the equimodular curve $|\kappa_+(z)| = |\kappa_-(z)|$.

3. There is a necklace on the left hand side which is "bisected" by the curve $|\kappa_+(z)| = |\kappa_-(z)|$.

4. Up through $L_h = 27$ the number of necklace regions is $L/3 - 4$ but $L_h = 24$ and $L_h = 30$ each have 4 regions. There is no conjecture for $L_h > 30$.

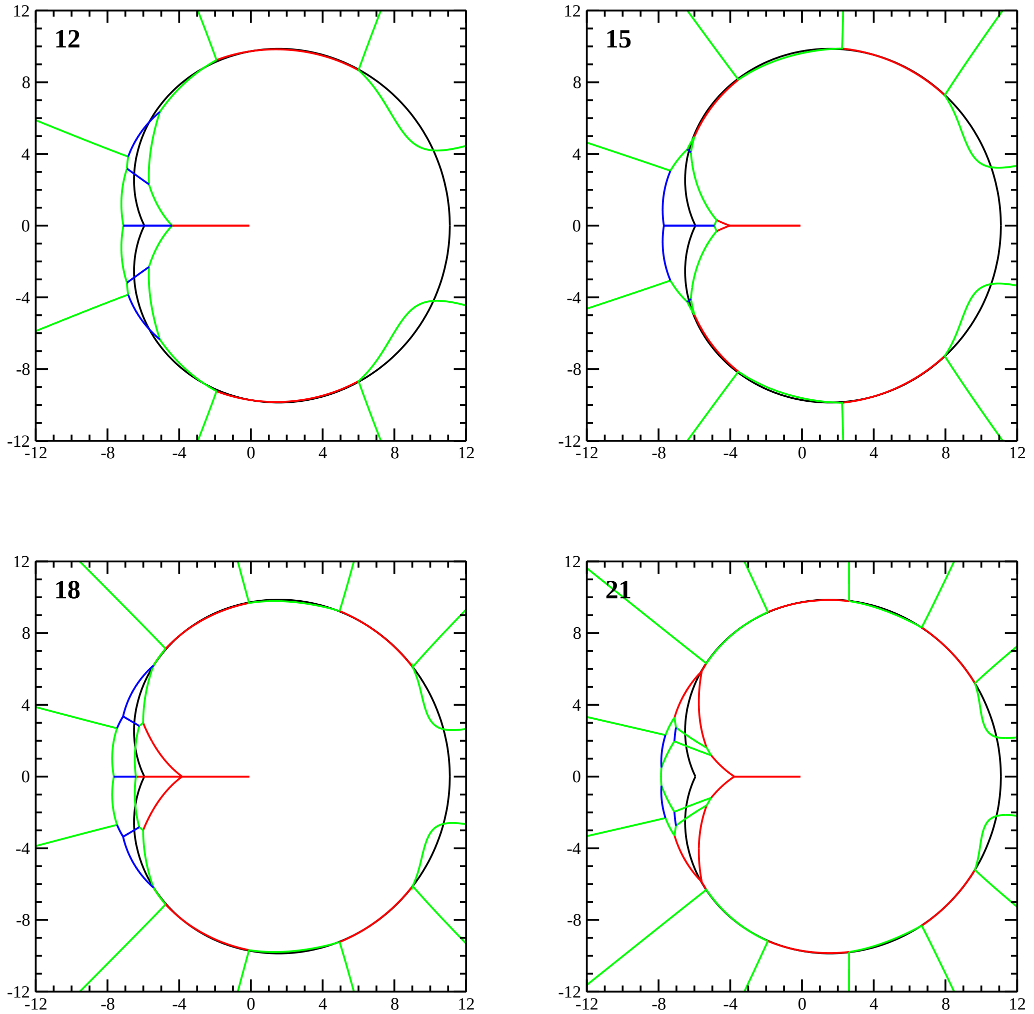

Equimodular curves of hard hexagon eigenvalues for toroidal lattices. Red = 2 eigenvalues; Green = 3 eigenvalues; Blue = 4 eigenvalues. The curve $|\kappa_-(z)| = |\kappa_+(z)|$ is black.

Comments

1.Only $P = 0, \pm 2\pi/3$ contribute

2. Rays to infinity
The rays which extend to infinity separate regions where the single eigenvalue at $P = 0$ is dominant from regions where the two eigenvalues with $P = \pm 2\pi/3$ are dominant. On these rays three eigenvalues have equal modulus.

3. Dominance of $P = 0$ as $L_h \to \infty$
As L_h increases the regions with $P = 0$ grow and squeeze the regions with $P = \pm 2\pi/3$ down to a very small area. It is thus most natural to conjecture that in the necklace, in the limit $L_h \to \infty$, only momentum $P = 0$ survives, except possibly on the equimodular curves themselves.

5. Hard hexagon partition function zeros

For cylindrical boundary conditions we have computed hard hexagon partition function zeros on $3L \times 3L$ lattices up to size $3L = 39$ and we compare them with equimodular curves by computing $27 \times 27,\ 27 \times 54,\ 27 \times 135,\ 27 \times 270.$

For toroidal boundary conditions we have computed partition function zeros on $3L \times 3L$ lattices for up to size $3L = 27$ and we compare them with equimodular curves by computing $15 \times 150,\ 15 \times 300,\ 15 \times 600,\ 18 \times 180,\ 18 \times 360,\ 21 \times 210.$

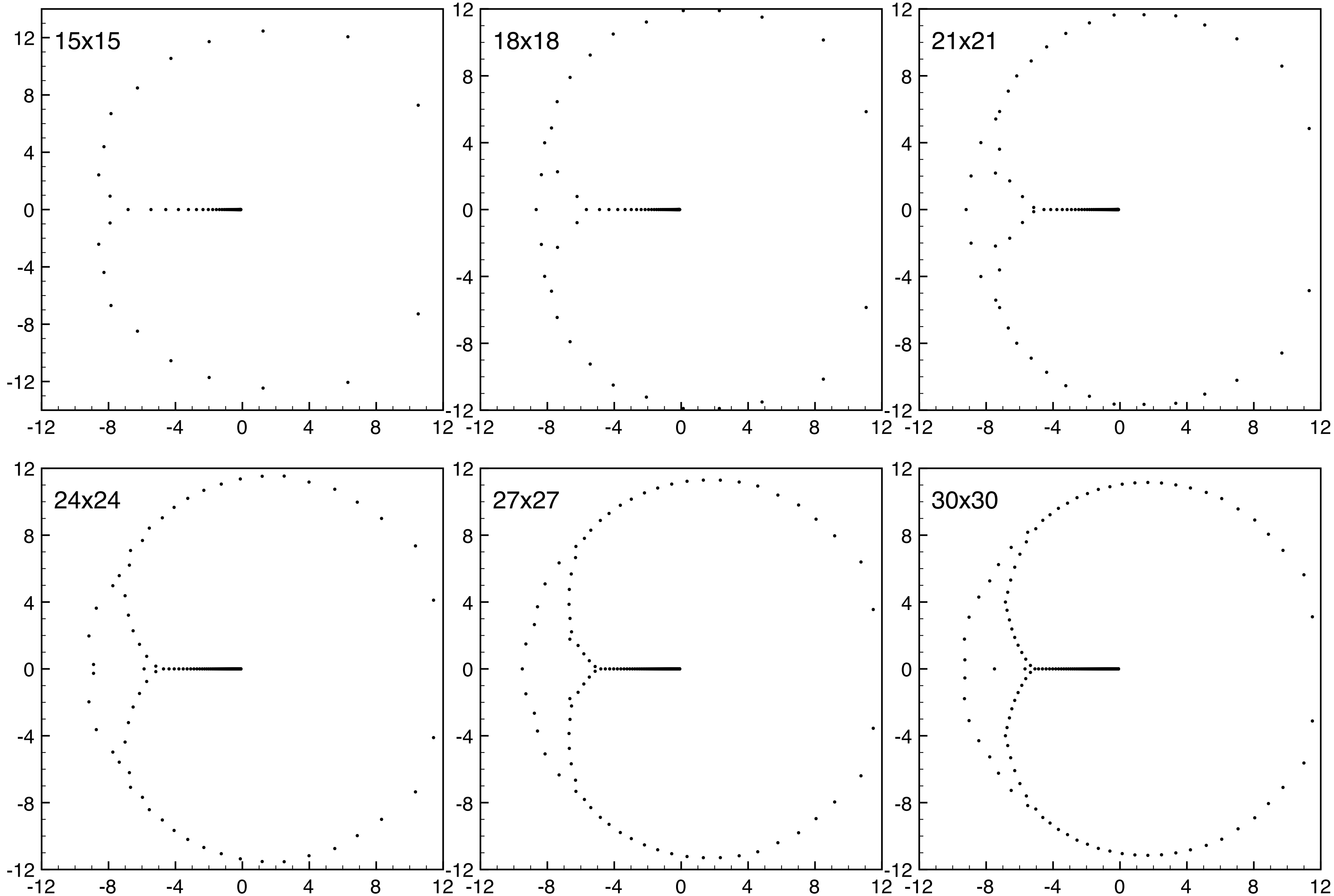

Partition function zeros of hard hexagons with cylindrical boundary conditions.

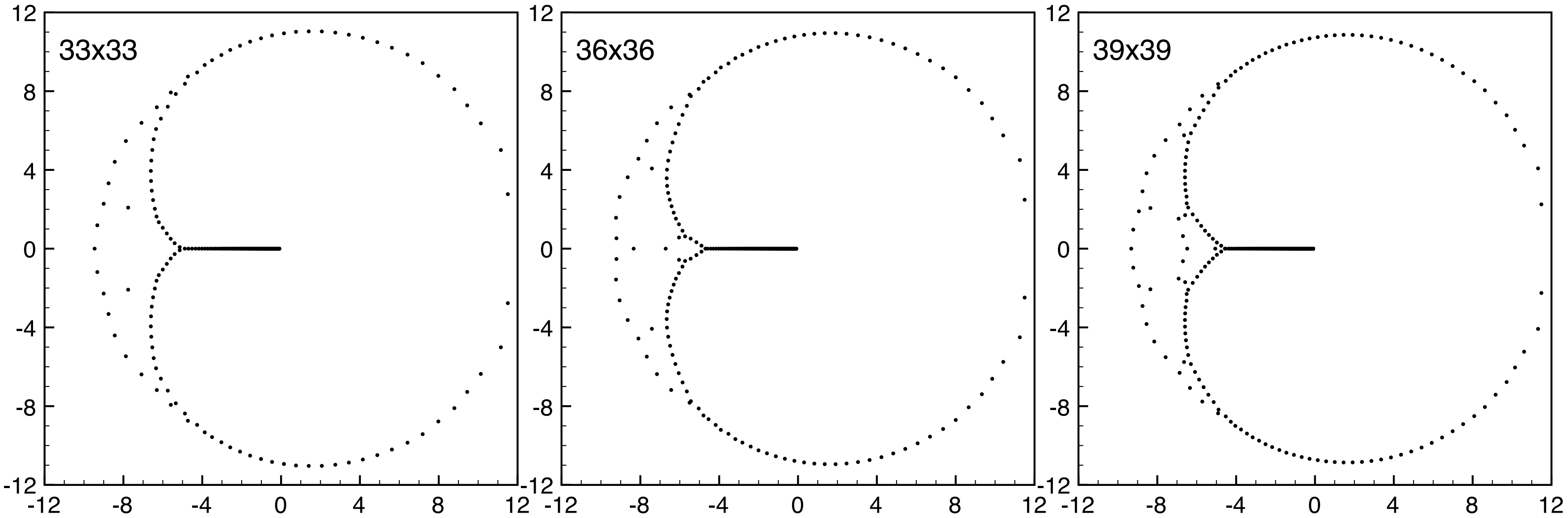

Partition function zeros of hard hexagons with cylindrical boundary conditions.

Comments

1. Starting with 30×30 zeros start to appear in the necklace and separated regions begin to be apparent.
2. For 36×36 it can be argued that there are 5 regions.
3. For 39×39 it can be argued that there are 7 regions.
4. It is unknown if as $L \to \infty$ the zeros fill the entire necklace region.

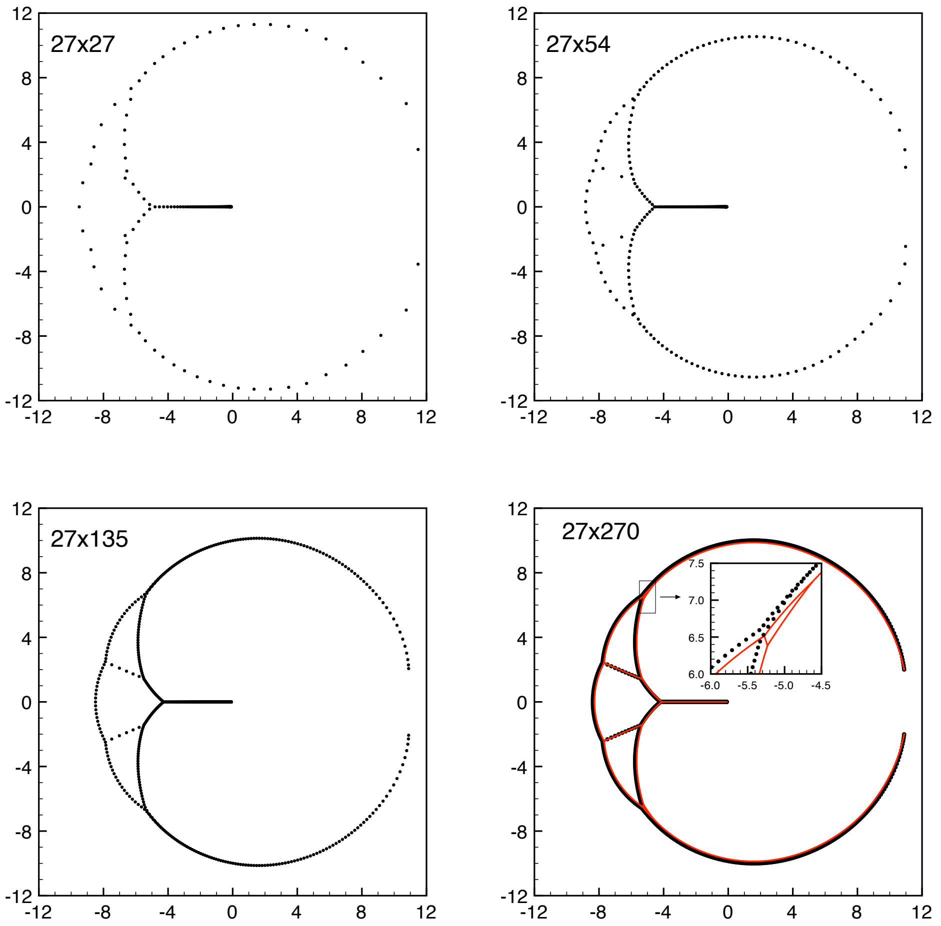

The partition function zeros for $L_h \times L_v$ cylindrical lattices. For 27×270 the equimodular eigenvalue curve is superimposed in red.

Comments

These plots illustrate a general phenomenon that what appears in the 27×27 plot as a very slight deviation from smooth curves develops for $L_h \times L_v$ with $L_v \to \infty$ into the lines separating regions seen in the equimodular plots.

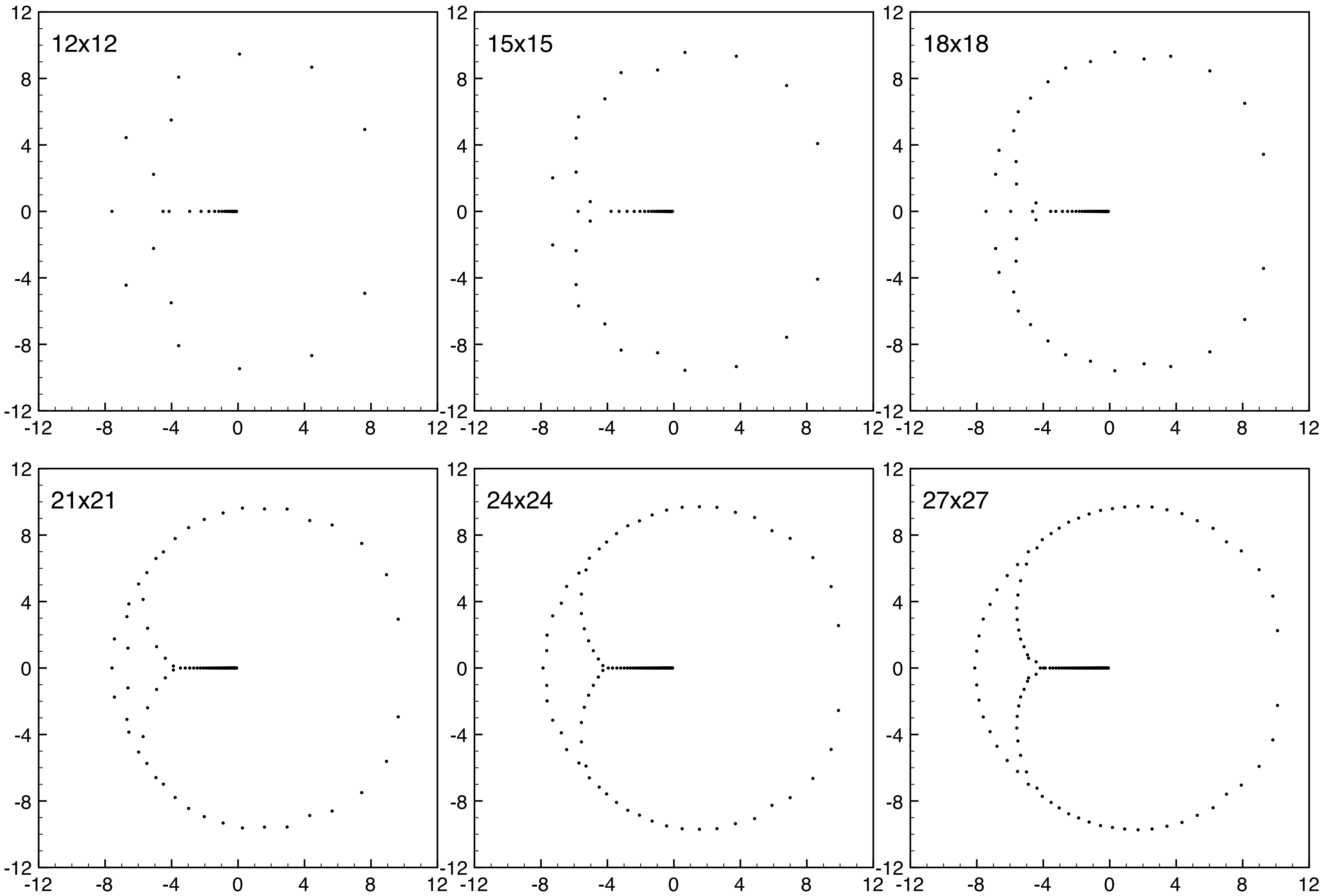

Partition function zeros for hard hexagon with toroidal boundary conditions of size $L \times L$.

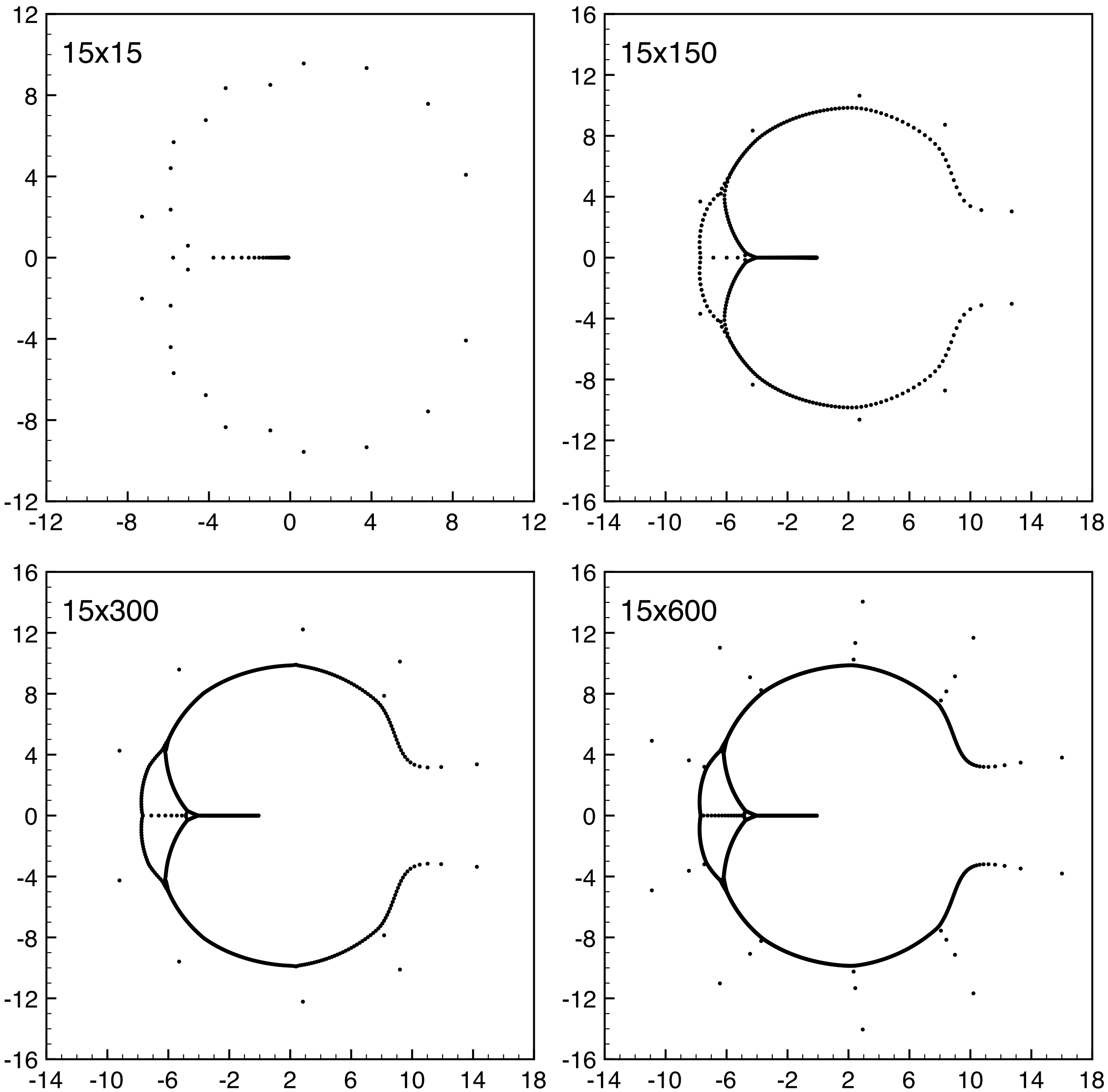

Partition function zeros for toroidal boundary conditions for some $15 \times L_v$ lattices.

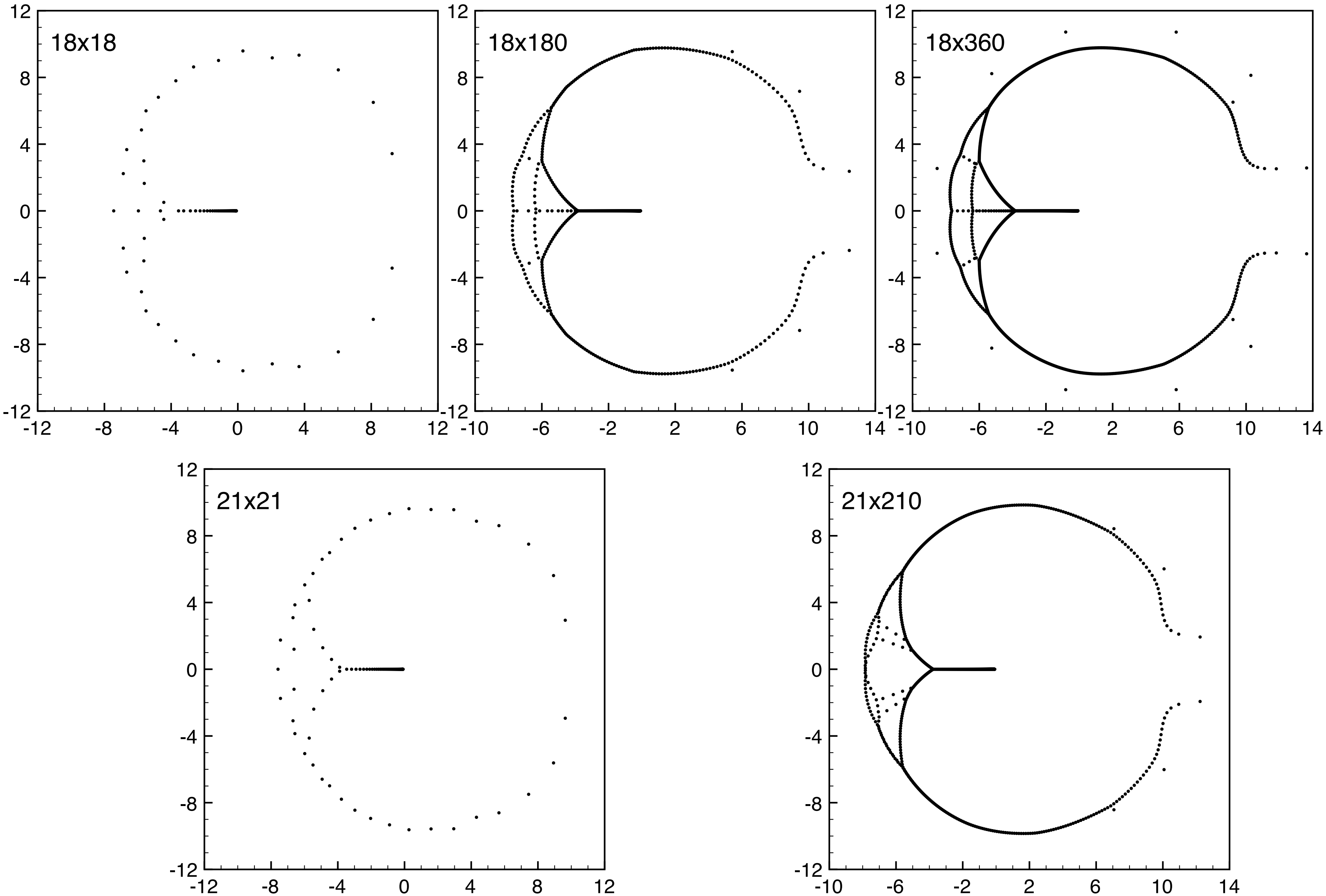

Partition function zeros for toroidal boundary conditions for some $18 \times L_v$ and $21 \times L_v$ lattices. The number of points off of the main curve for fixed aspect ratio L_v/L_h decreases with increasing L_h.

Density of zeros $D(z)$ for $z < z_d$

$$D(z) = \lim_{L\to\infty} D_L(z_j) \quad \text{where}$$
$$D_L(z_j) = \frac{1}{N_L \cdot (z_j - z_{j+1})}.$$

As $z \to z_d$, $D(z)$ diverges as $(1 - z/z_d)^{-1/6}$

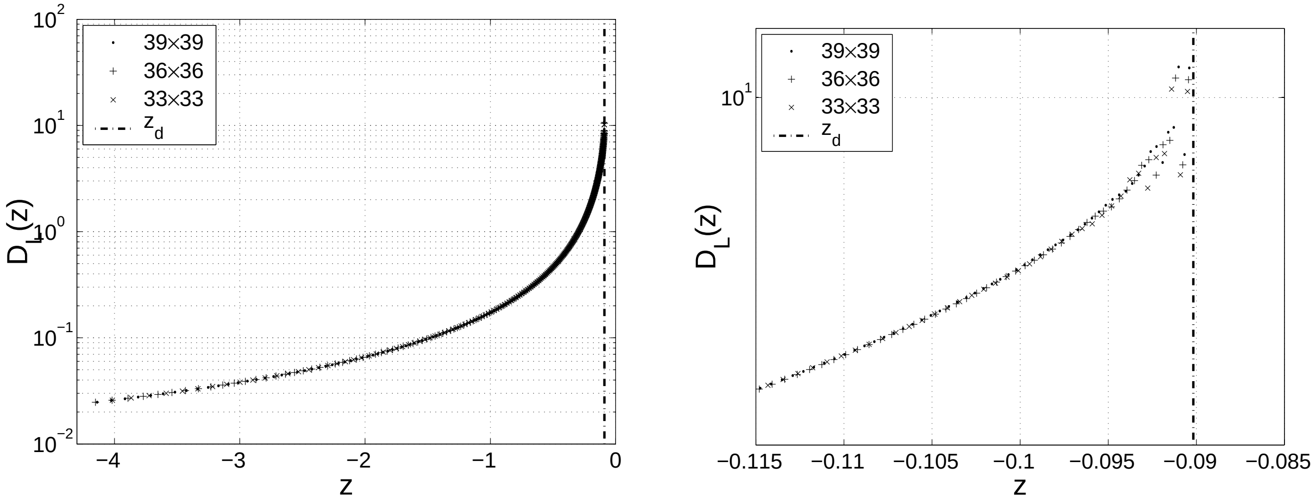

Log plots of the density of zeros $D_L(z_j)$ on the negative z axis for $L \times L$ lattices with cylindrical boundary conditions. The figure on the right is an expanded scale near the singular point z_d.

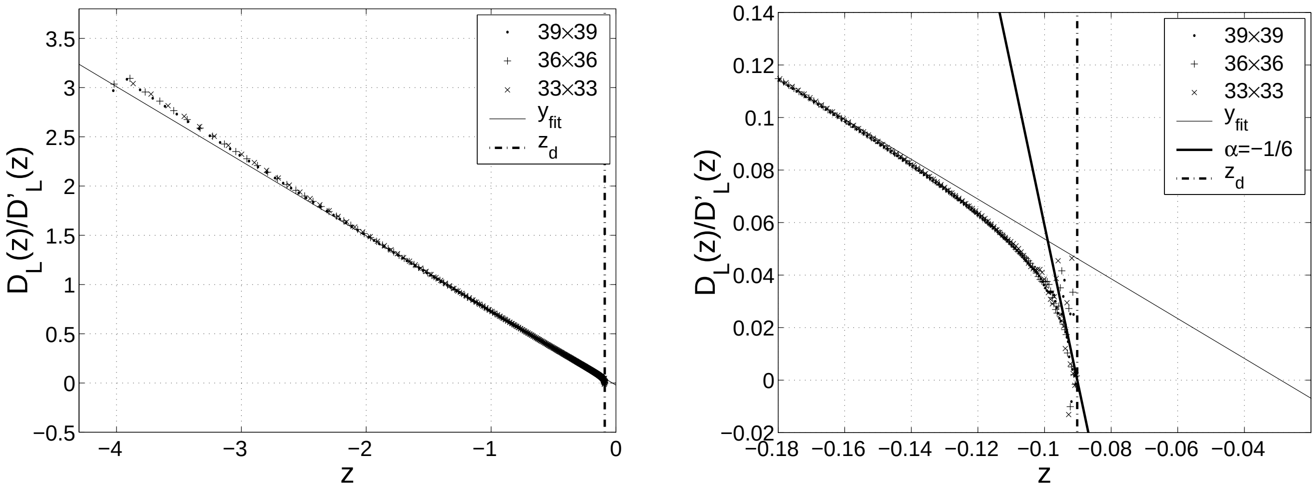

Plots of $D_L(z_j)/D'_L(z_j)$ on the negative z axis for $L \times L$ lattices with cylindrical boundary conditions.

For the plot on the left for the range $-4.0 \le z \le -0.14$ the data is extremely well fitted by the power law form with an exponent -1.32 and an intercept $z_f = -0.029$. The plot on the right is an expanded scale near z_d and the line passing through $z = z_d$ corresponds to the true exponent $= -1/6$ which only is observed in a very narrow range near z_d of $-0.095 \le z \le z_d = -0.0901 \cdots$.

6. Hard square zeros

For cylindrical boundary conditions we have computed partition function zeros on $2L \times 2L$ lattices up to size $2L = 38$.

For toroidal boundary conditions we have computed partition function zeros on $2L \times 2L$ lattices for up to size $2L = 28$.

For cylindrical boundary conditionswe study the dependence on aspect ratio L_v/L_h by computing partition function zeros on $26 \times L_v$ lattices up to $L_v = 260$.

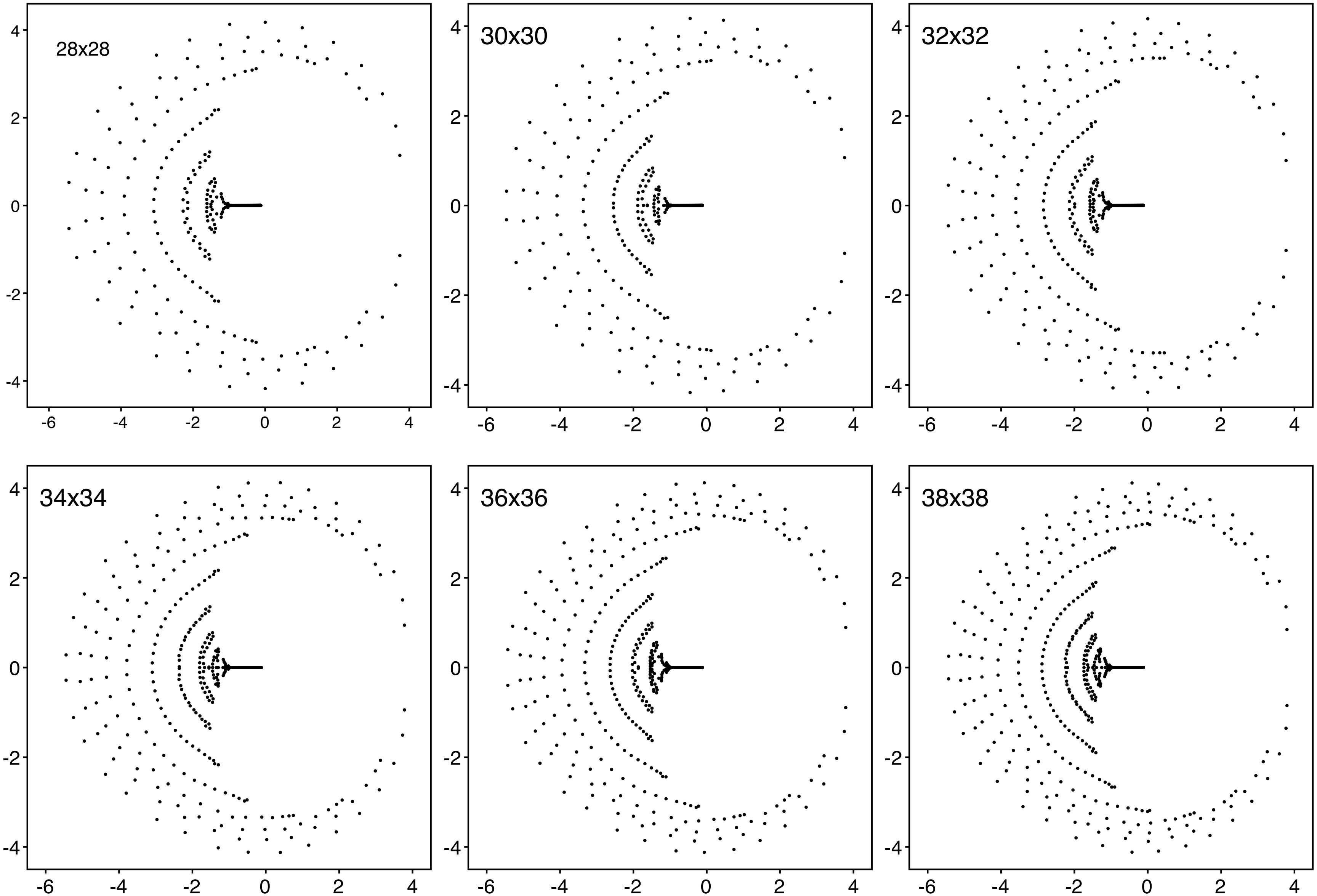

Partition function zeros of hard squares with cylindrical boundary conditions.

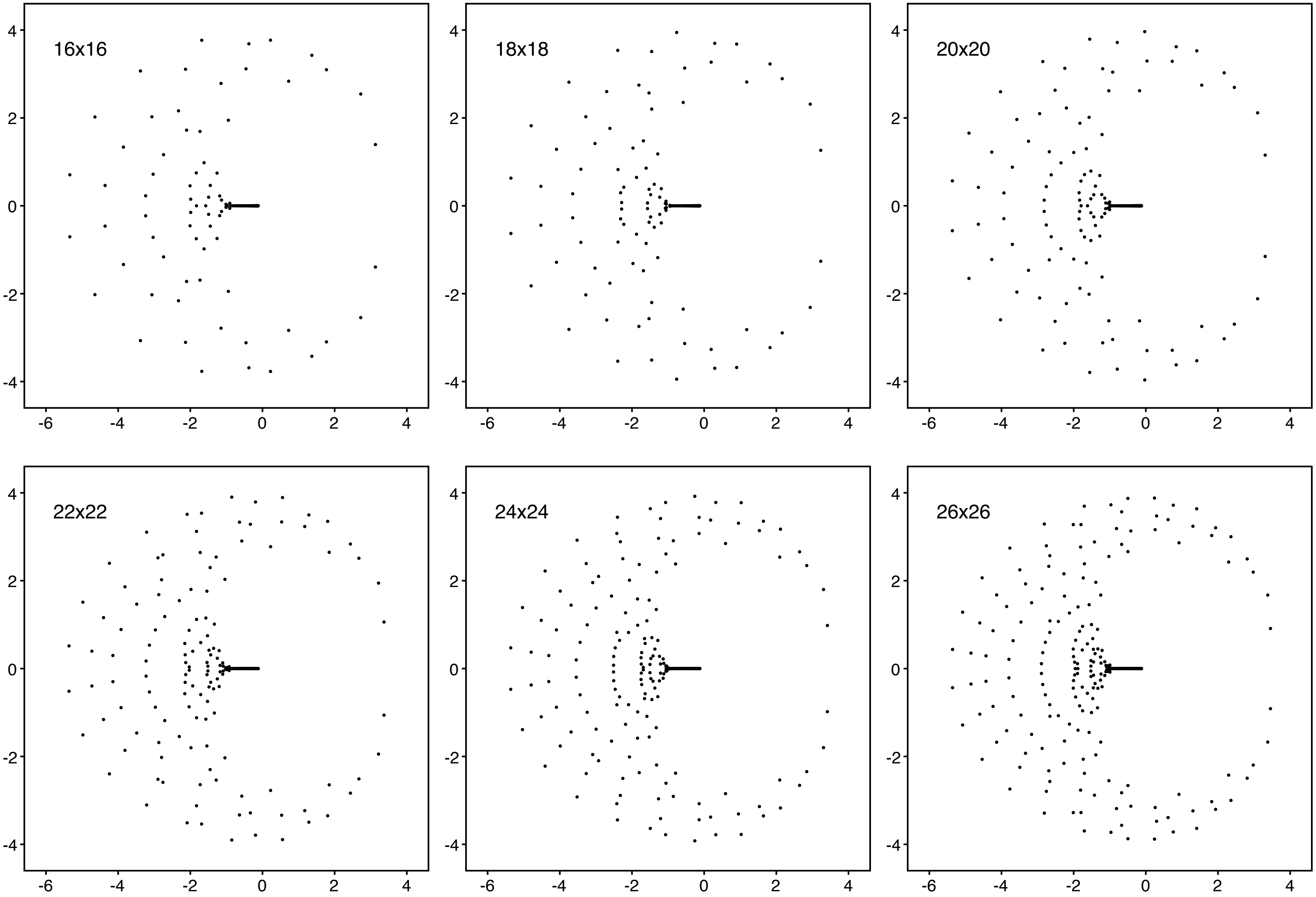

Partition function zeros of hard squares with toroidal boundary conditions.

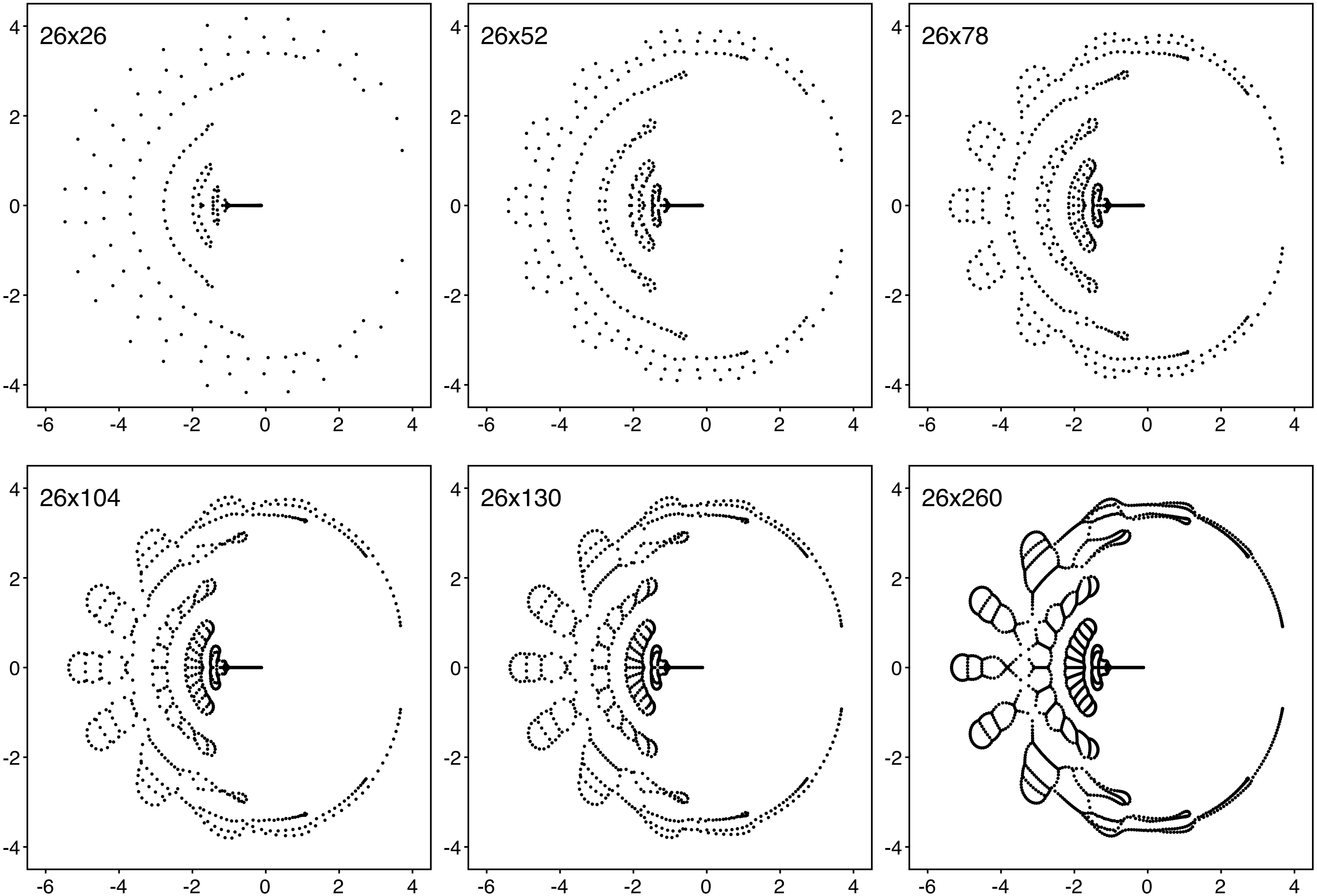

Partition function zeros of hard squares with cylindrical boundary conditions on $26 \times L_v$ lattices.

Gaps on $-1 < z < z_d$

The maximum eigenvalue is real for $z_r < z < z_l$ where z_r and z_l are roots of the resolvant of the characteristic equation.

L_h	z_r	z_l	gap
6	-0.4783	-0.52383	0.04900
8	-0.30373	-0.30603	0.00230
10	-0.23722	-0.23736	1.4×10^{-4}
	-0.73653	-0.77923	0.04270
12	-0.204004	-0.204016	1.2×10^{-5}
	-0.49353	-0.49533	0.00180
14	-0.1846428	-0.1846440	1.2×10^{-6}
	-0.37181	-0.37193	1.2×10^{-4}
	-0.9195	-0.9255	0.0060

Gaps on $-1 < z < z_d$

16	-0.1721143	-0.17211444	1.4×10^{-7}
	-0.305078	-0.305086	8×10^{-6}
	-0.64204	-0.64336	0.00132
18	-0.163388998	-0.163389012	1.4×10^{-8}
	-0.2643045	-0.2643054	9×10^{-7}
	-0.494388	-0.494482	9.4×10^{-5}
20	-0.156991029	-0.156991031	2×10^{-9}
	-0.2237253	-0.23723539	9×10^{-8}
	-0.404120	-0.404127	7×10^{-6}
	-0.7523	-0.7537	0.0014

7. Square Ising in a field

The Ising model on a square lattice in a magnetic field H is defined by
$\mathcal{E} = -E\sum_{j,k}\{\sigma_{j,k}\sigma_{j+1,k} + \sigma_{j,k}\sigma_{j,k+1}\} - H\sum_{j,k}\sigma_{j,k}$.

We use the notation

$x = e^{-2H/kT}$ and $y = x^{1/2}e^{-4E/kT}$

Hard squares $z = \lim_{x\to 0, E\to -\infty} y^2$

Ising at $H = 0$ is $x = 1$.

The partition zeros have been computed on the 20×20 lattice.

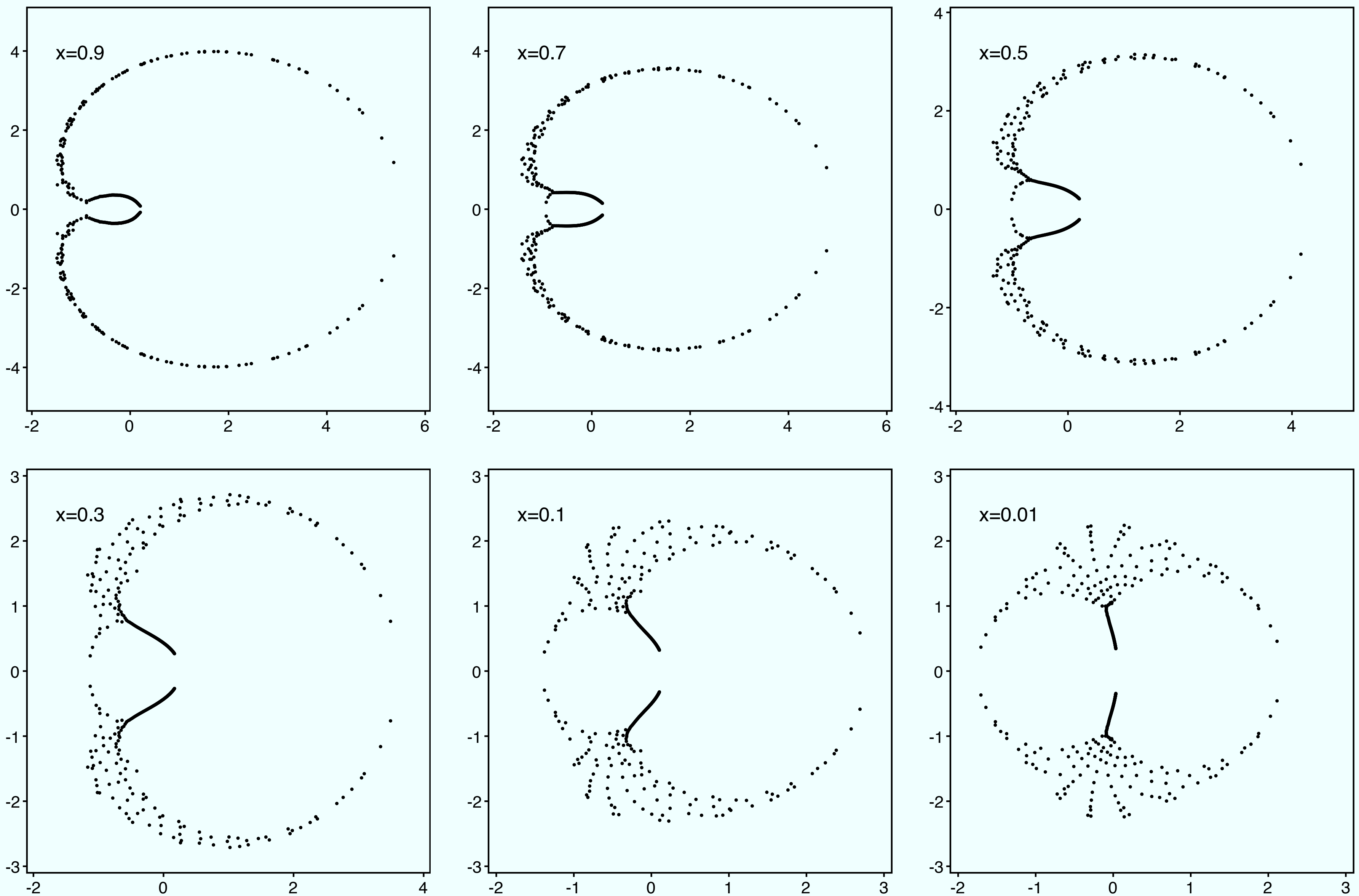

Zeros for the 20×20 square Ising lattice for $x = e^{-2H/kT}$ in the plane of complex $y = e^{-H/kT} e^{-4E/kT}$.

Universality

Universality says (in some rather vague way) that the behaviors at the following points are the same

z_d of hard hexagons

z_d of hard squares

The “ferromagnetic” complex singularity of Ising at $H \neq 0$

The sigularity at the Lee=Yang edge.

Does this chain of reasoning connect the natural boundary of Nickel with the analyticity of hard squares for $-1 < z < z_d$ and with analyticity of the Lee-Yang arc?

8. Further open questions

1. If for hard squares the real gaps become dense on $-1 < z < z_d$ will this prevent analytic continuation in the thermodynamic limit?

2. Is there any meaning to the great structure seen in the hard square zeros?

3. What is the implication that for hard squares all eigenvalues are equimodular at $z = -1$?

4. Neither the zeros nor the equimodular curves approach z_c on the positive real axis as a single curve. What does this imply about analyticity at z_c?

5. There are only three "endpoints" in the 26×260 zero plots. Does this affect analyticity at z_c?

6. The expansion of $\rho_-(z)$ for hard squares at z_d is expected by renormalization and universality arguments to have the same form as the hard hexagon expansion. Will the infinite series which multiply each of the six exponents converge?

7. Does the non generic factorization of the characteristic equation in the $P = 0$ sector for hard hexagons imply that the analyticity properties of hard hexagons are not generic?

8. What is the thermodynamic limit of the necklace region for hard heagons?

9. Conclusion

I am fond of the following theorem from philosophy

No one can be said to understand a paper until and unless they can generalize it.

A corollary to this theorem is that

No author understands their most recent paper

This talk well illustrates this corollary